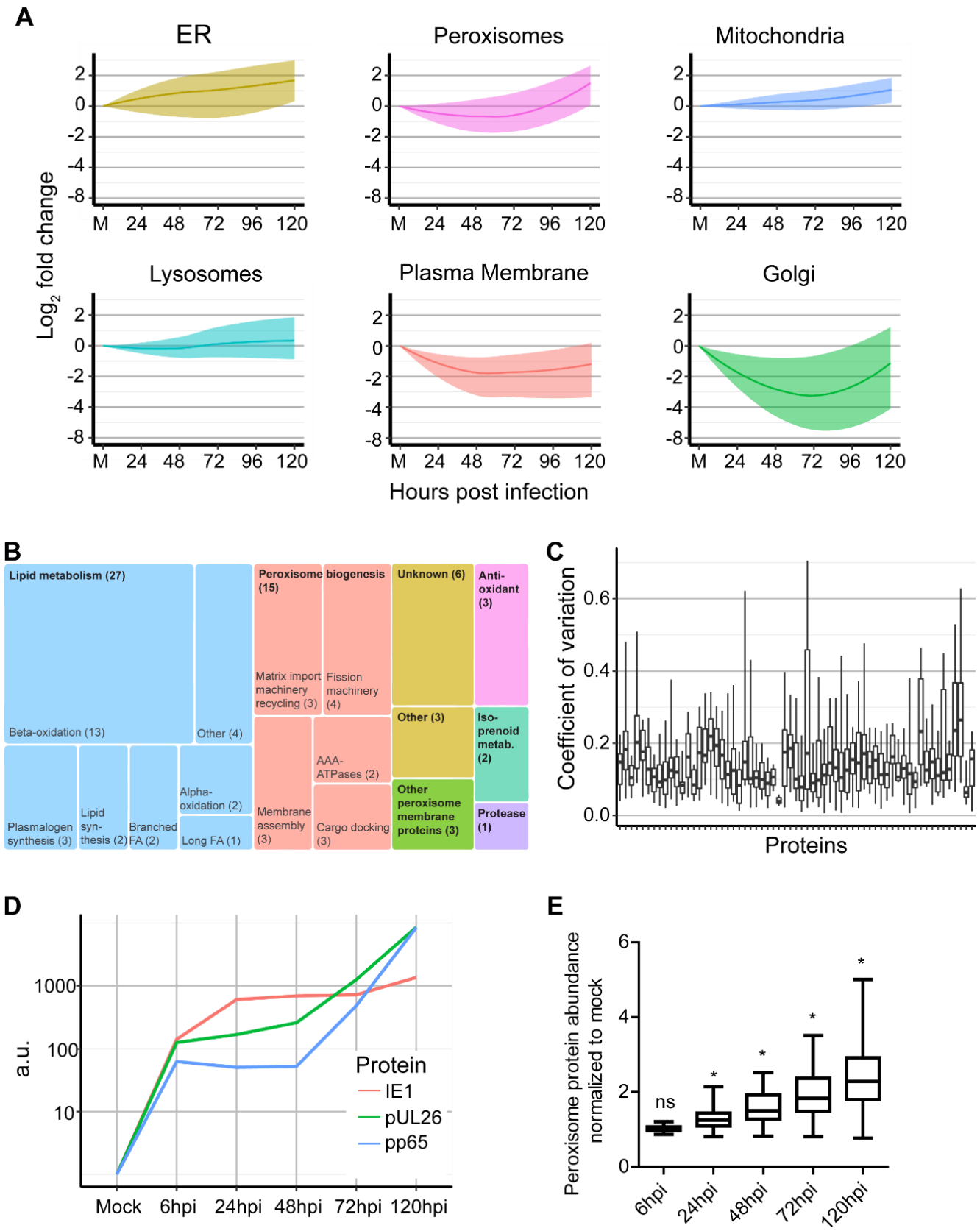
A
ER
Peroxisomes
Mitochondria
Lysosomes
Plasma Membrane
Golgi
Log2 fold change
Hours post infection
M 24 48 72 96 120
2 0 -2 -4 -8
B
Lipid metabolism (27)
Beta-oxidation (13)
Other (4)
Plasmalogen synthesis (3)
Lipid syn-thesis (2)
Branched FA (2)
Alpha-oxidation (2)
Long FA (1)
Peroxisome biogenesis (15)
Matrix import machinery recycling (3)
Fission machinery (4)
AAA-ATPases (2)
Membrane assembly (3)
Cargo docking (3)
Unknown (6)
Other (3)
Other peroxisome membrane proteins (3)
Anti-oxidant (3)
Iso-prenoid metab. (2)
Protease (1)
C
Coefficient of variation
0.0 0.2 0.4 0.6
Proteins
D
a.u.
10 100 1000
Mock 6hpi 24hpi 48hpi 72hpi 120hpi
Protein
IE1
pUL26
pp65
E
Peroxisome protein abundance normalized to mock
0 2 4 6
ns
*
6hpi 24hpi 48hpi 72hpi 120hpi

Figure S1. Data quality assessment and additional analyses of the peroxisome proteome quantification during HCMV infection. Related to Fig 1.

A) Means (solid lines) and inter-quartile ranges (shades) of organelle proteomes throughout the infectious cycle from data collected in our previous proteomic study (Jean Beltran et al., 2016). Note that the magnitude of this increase late in infection was similar to the functionally-relevant HCMV-induced increases in ER and mitochondria protein abundances

B) Tree map showing the number of proteins quantified from different peroxisome functional categories. Categories are shown in bold colored fonts and subcategories in normal font with numbers indicating the number of proteins.

C) Boxplots summarizing the coefficient of variation of individual peptides from all samples (n=18) across replicates. Boxes show inter-quartile range (IQR) and whiskers show the full range of values.

D) Abundance of viral proteins from three viral genes representing IE (UL123), DE (UL26), and L (UL83) kinetic classes. Y-axis is shown in a log10 scale. Note that the abundances detected in the mock sample were at background level for all three proteins

E) Boxplots summarizing the abundance of all peroxisome proteins detected by PRM relative to mock. Boxes show inter-quartile range (IQR) and whiskers show the full range of values. ANOVA followed by Dunn's multiple comparison test was used to assess significant changes relative to mock (ns, not significant; * $p<0.05$)

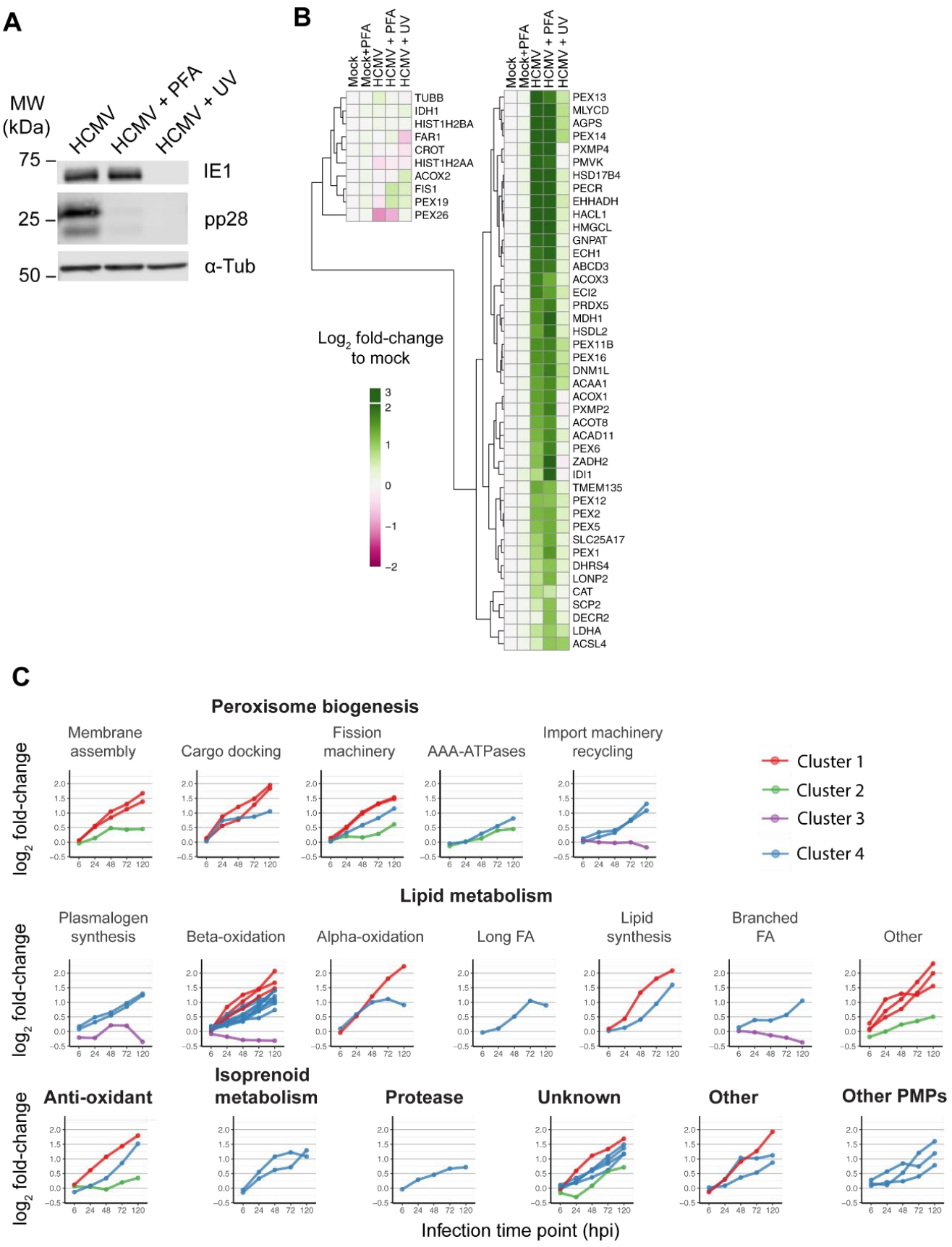
A
MW (kDa)
HCMV
HCMV + PFA
HCMV + UV
75 –
25 –
50 –
IE1
pp28
α-Tub
B
Mock
Mock+PFA
HCMV
HCMV + PFA
HCMV + UV
TUBB
IDH1
HIST1H2BA
FAR1
CROT
HIST1H2AA
ACOX2
FIS1
PEX19
PEX26
PEX13
MLYCD
AGPS
PEX14
PXMP4
PMVK
HSD17B4
PECR
EHHADH
HACL1
HMGCL
GNPAT
ECH1
ABCD3
ACOX3
ECI2
PRDX5
MDH1
HSDL2
PEX11B
PEX16
DNM1L
ACAA1
ACOX1
PXMP2
ACOT8
ACAD11
PEX6
ZADH2
IDI1
TMEM135
PEX12
PEX2
PEX5
SLC25A17
PEX1
DHRS4
LONP2
CAT
SCP2
DECR2
LDHA
ACSL4
Log2 fold-change to mock
3
2
1
0
−1
−2
C
Peroxisome biogenesis
Membrane assembly
Cargo docking
Fission machinery
AAA-ATPases
Import machinery recycling
Cluster 1
Cluster 2
Cluster 3
Cluster 4
Lipid metabolism
Plasmalogen synthesis
Beta-oxidation
Alpha-oxidation
Long FA
Lipid synthesis
Branched FA
Other
Anti-oxidant
Isoprenoid metabolism
Protease
Unknown
Other
Other PMPs
log2 fold-change
Infection time point (hpi)

Figure S2. Temporal kinetics and functions associated with peroxisome protein abundances during HCMV infection. Related to Fig 1.

A) Western blot analysis of immediate early (IE1) and late (pp28) viral gene expression in infected cells treated with phosphonoformate (PFA) or with cells infected with UV-inactivated virus at 120 hpi. Tubulin used as loading control.

B) Heatmap of peroxisome protein abundance in uninfected (Mock), uninfected with PFA treatment (Mock+PFA), 120hpi with normal HCMV (HCMV), 120hpi during PFA treatment (HCMV + PFA), and 120hpi with UV-inactivated HCMV (HCMV + UV).

C) Log_2 fold-change abundance values of peroxisome proteins through infection. Proteins were grouped according to their functions. Colors indicate 4 clusters obtained by hierarchical clustering (Fig 1C).

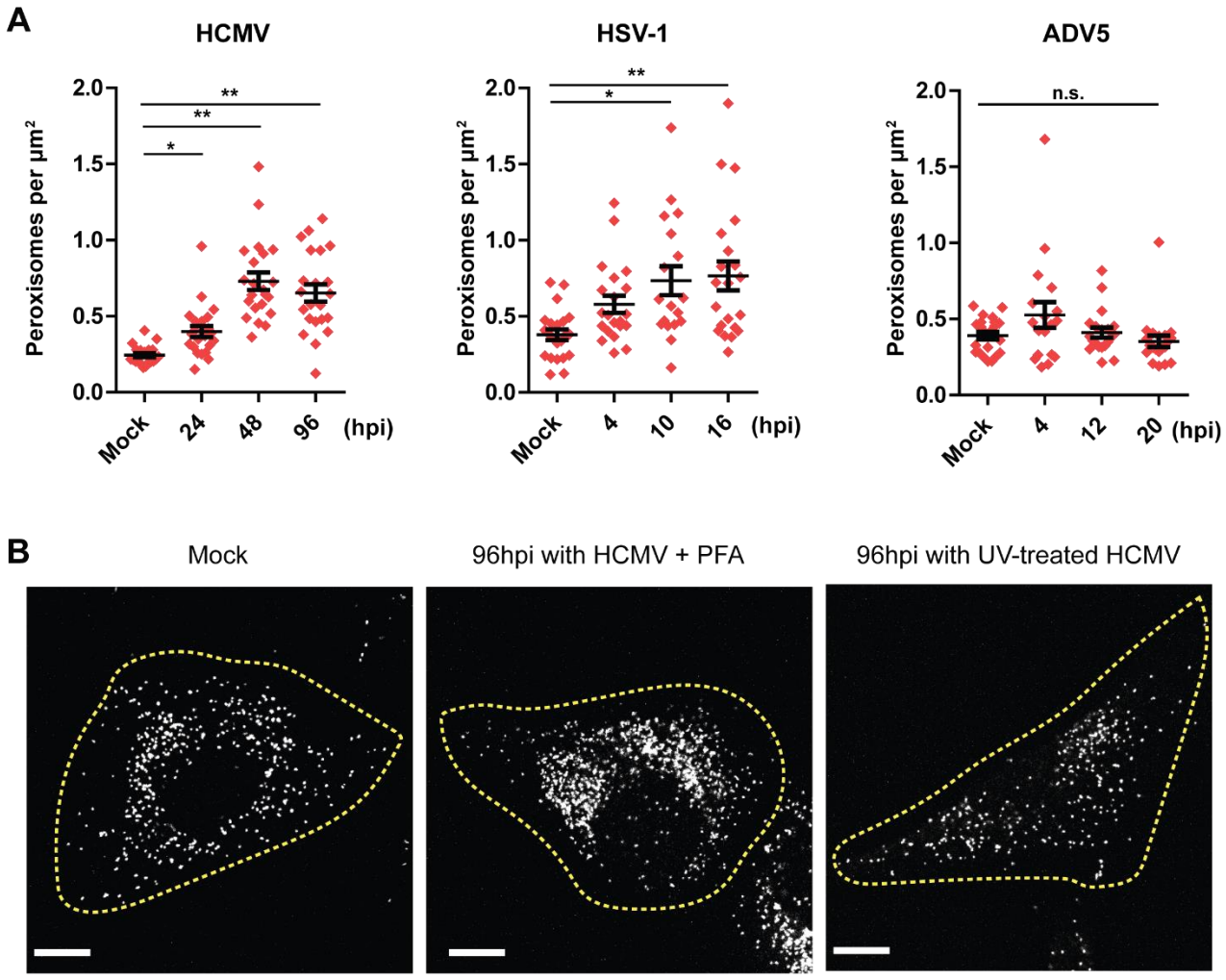

Figure S3. Peroxisome abundance in infected cells during PFA treatment. Related to Figure 2.

A) Peroxisome numbers normalized to cell area in µm^2 shown for cells infected with HCMV (left), HSV-1 (middle), or ADV5 (right) at the indicated time points after infection. Statistical significance marked with (*) for P<0.05, and (**) for P<0.01.

B) IF analysis of peroxisomes using anti-PEX14 from HFs either uninfected (left), infected and treated with PFA (middle), or infected with UV-irradiated viruses (right). Scale bar = 10µm.

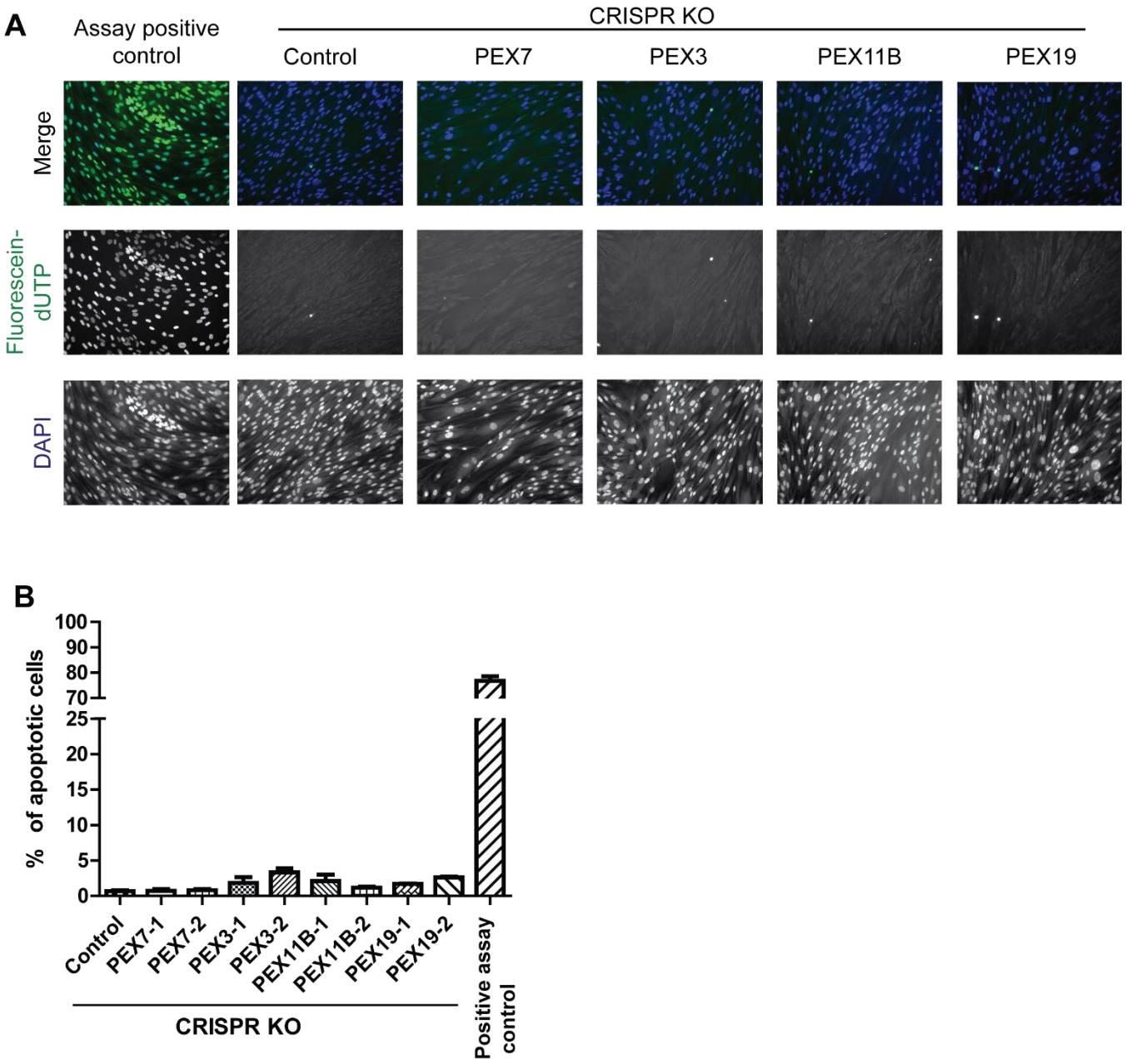

Figure S4. Viability of CRISPR KO cell lines. Related to Figure 3.

A) Cell viability was assessed by TUNEL assay through detection of DNA breaks using fluorescein-dUTP. As positive control, DNA breaks were induced with DNase I.

B) Percent of apoptotic cells across CRISPR KO cell lines and non-targeting CRISPR control.

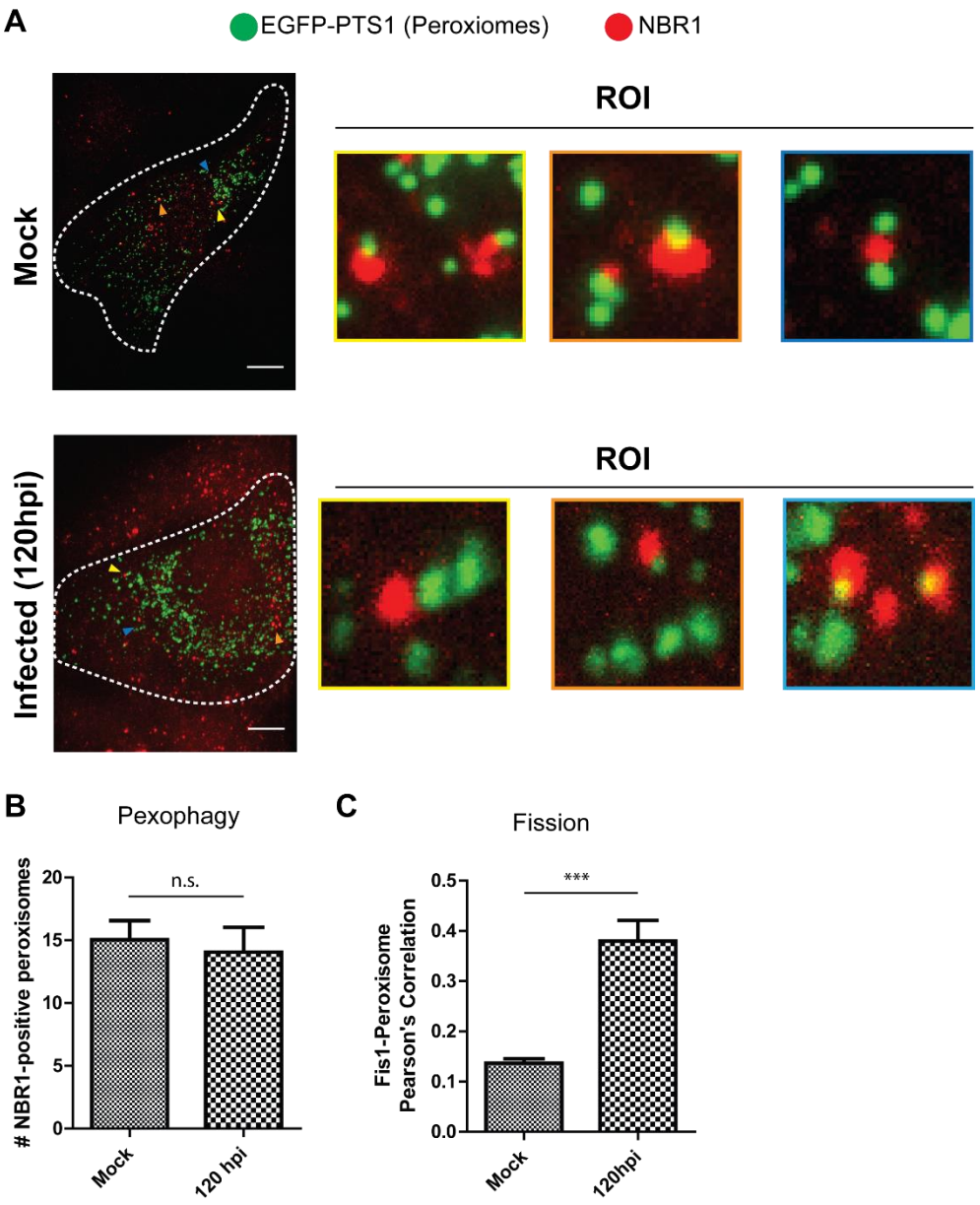

Figure S5. Pexophagy analysis during HCMV infection. Related to Figure 4.

A) Immunofluorescence analysis of NBR1 and peroxisomes EGFP-PTS1 in uninfected (Mock) and infected at 120hpi. ROIs show examples of NBR1 association with peroxisomes. Scale bars represent 10µm.

B) Number of NBR1-positive peroxisomes were counted in uninfected or infected cells. N > 15 cells.

C) Data as in Fig 4G showing colocalization of Fis1 with peroxisomes in uninfected and infected (120 hpi) conditions for comparison. N > 10 cells. Statistical significance determined by t-test and marked with (*) for P<0.05, (**) for P<0.01, (***) for P<0.001, or n.s. for no statistical significance.

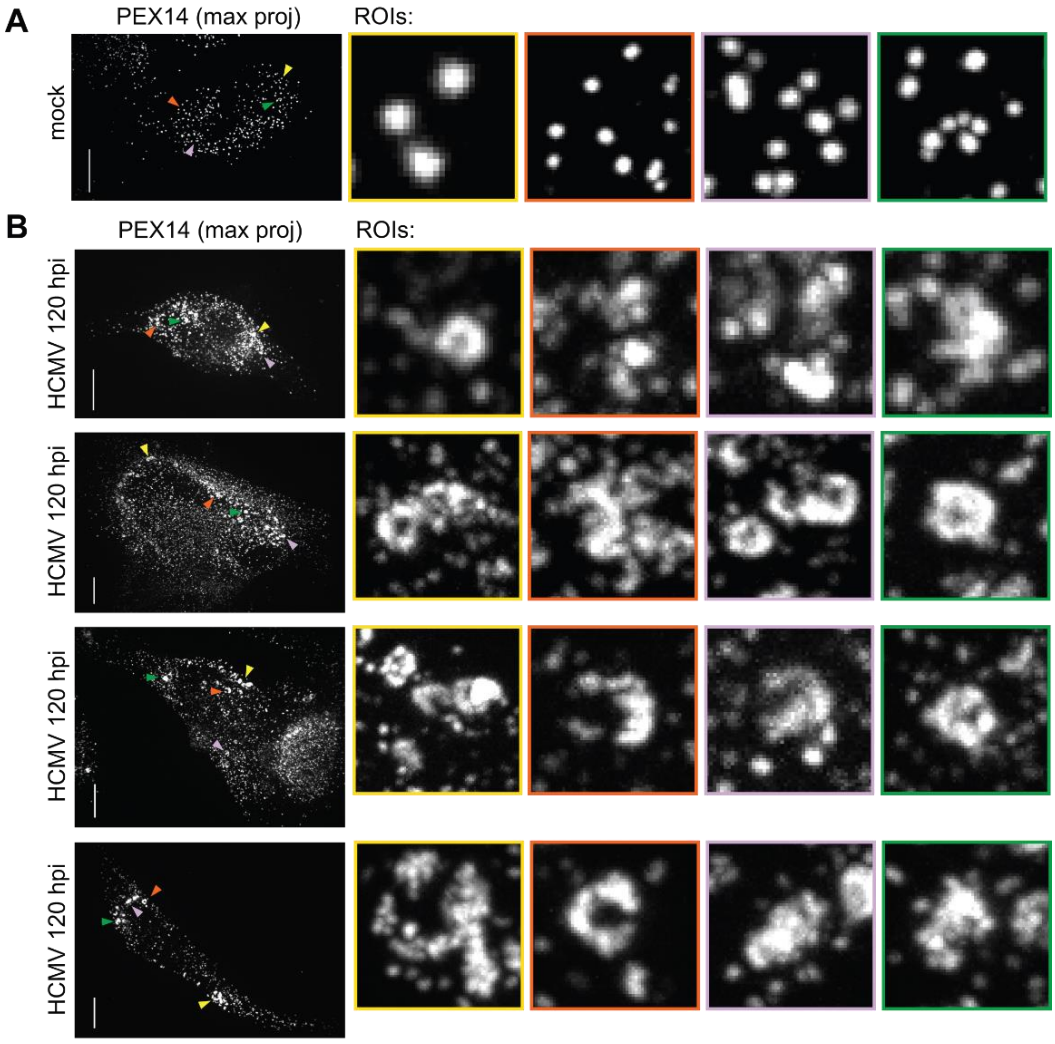
A
PEX14 (max proj)
ROIs:
mock
B
PEX14 (max proj)
ROIs:
HCMV 120 hpi
HCMV 120 hpi
HCMV 120 hpi
HCMV 120 hpi

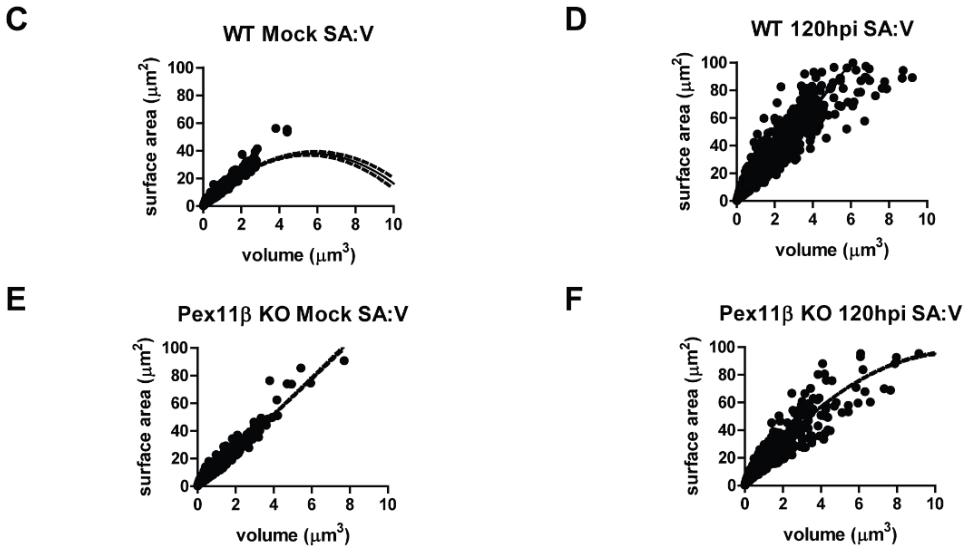
C
WT Mock SA:V
surface area (μm²)
volume (μm³)
D
WT 120hpi SA:V
surface area (μm²)
volume (μm³)
E
Pex11β KO Mock SA:V
surface area (μm²)
volume (μm³)
F
Pex11β KO 120hpi SA:V
surface area (μm²)
volume (μm³)

Figure S6. HCMV infection disrupts peroxisome shape and size. Related to Figure 5.

A-B) Maximum projections of A) mock and B) HCMV-infected cells at 120hpi labelled with anti-PEX14 and imaged at 100X. Arrowheads indicate ROIs in the corresponding color. Scale bars represent 10µm.

C-F) Plot of the surface area and volume of individual peroxisomes in (C) uninfected wild type (WT) cells (mean SA:V = 21.4 μm^{-1}), (D) WT cells 120 hpi (mean SA:V = 31.04 μm^{-1}), (E) uninfected PEX11B KOs (mean SA:V = 21.3 μm^{-1}), (F) PEX11B KOs, 120 hpi (mean SA:V = 30.2 μm^{-1}). Solid line indicates the regression curve, dashed lines indicate the upper and lower 95% confidence intervals. N = 23868 peroxisomes in WT Mock; N = 33958 in WT 120 hpi; N = 7391 in Pex11B KO Mock; N = 16708 in Pex11B KO 120 hpi.

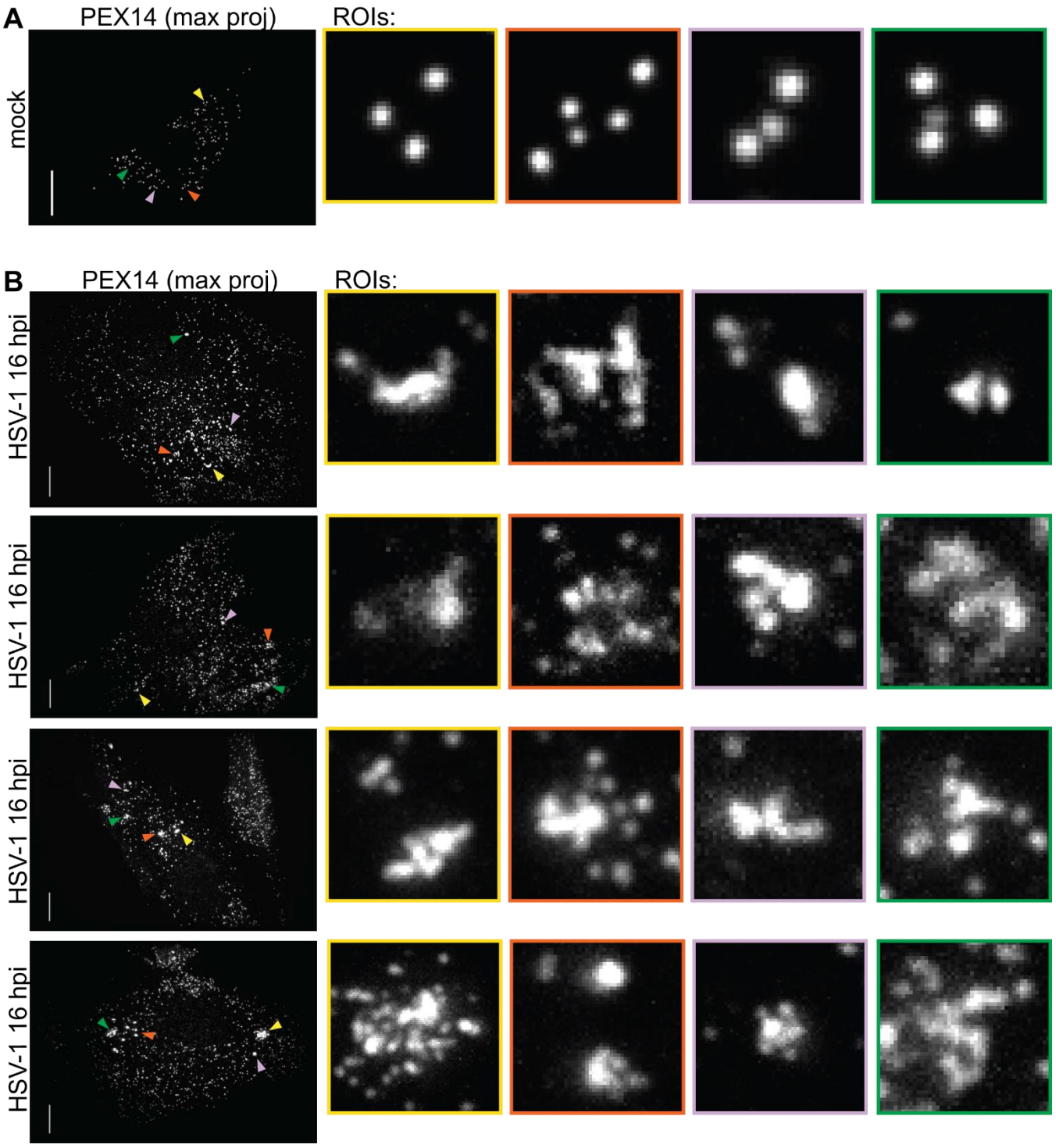

Figure S7. HSV-1 infection disrupts peroxisome shape and size. Related to Figure 6.

Maximum projections of A) mock and B) HSV1-infected cells at 16hpi labelled with anti-PEX14 and imaged at 100X. Arrowheads indicate ROIs in the corresponding color. Scale bars represent 10µm.